α-Conotoxin Residues that Interact at Close Range with γ-Tyrosine-111 and Mutant δ-Tyrosine-113 on the *Torpedo* Nicotinic Acetylcholine Receptor†

Wanda Vélez-Carrasco, Sonia Valdés, Lyann Agresar, Alyssa Lettich, Astrid Y. Guerra, and Richard M. Hann*

Department of Biochemistry and Center for Molecular and Behavioral Neuroscience, Universidad Central del Caribe, Bayamón, Puerto Rico 00960

Received November 30, 2003; Revised Manuscript Received July 20, 2004

ABSTRACT: The α-conotoxins MI and GI display stronger affinities for the αγ agonist site on the *Torpedo californica* electrocyte nicotinic acetylcholine receptor (ACHR) than for the αδ agonist site, while α-conotoxin SI binds with the same affinity to both sites. Prior studies reported that the arginine at position 9 on GI and the tyrosine at position 111 on the receptor γ subunit were responsible for the stronger αγ affinities of GI and MI, respectively. This study was undertaken to determine if the α-conotoxin midchain cationic residues interact with *Torpedo* γY111. The findings show that lysine 10 on MI is responsible for the αγ selectivity of MI and confirm the previously reported importance of R9 on GI and on the SI analogue, SIP9R. The results also show that γY111 contributes substantially to the selective αγ high affinity of all three peptides. Double-mutant cycle analyses reveal that, in the αγ site, K10 on MI and R9 on SIP9R interact with the aromatic ring of γY111 to stabilize the high-affinity complex, while in contrast, R9 on GI does not. The substitution of Y for R at position 113 on the δ subunit converts the αδ site into a high-affinity site for MI, GI, and SIP9R through the interacting of δY113 with K10 on MI and with R9 on both GI and SIP9R. The overall data show that the residues in the two sites with which MI interacts, other than at γ111/δ113, are either the same or similar enough to exert equivalent effects on MI, indicating that MI binds in the same orientation at the αγ and αδ sites. Similar findings show that SIP9R probably also binds in the same orientation at the wild-type αγ and αδ sites. The finding that R9 on GI interacts closely with δR113Y but not with γY111 means that GI binds in different orientations at the αγ and αδ sites. This report also discusses the molecular basis of the difference in the MI high-affinity sites on *Torpedo* and embryonic mouse muscle ACHRs.

The nicotinic acetylcholine receptor (ACHR)[1] from *Torpedo californica* electric organ is a pentameric transmembrane protein, which has a subunit stoichiometry of $\alpha_2\beta\gamma\delta$ and forms an agonist-gated cation channel through the membrane (*1*). Like all muscle-type ACHRs, each *Torpedo* receptor molecule has two nonidentical agonist-binding sites, which are located in the extracellular domain at the αγ and αδ subunit interfaces (*1*, *2*). The α subunits contribute three segments or "loops", which are centered near αY93 (loop A), αW149 (loop B), and αY190−Y198 (loop C), while the γ and δ subunits contribute four segments, which are centered near γK34/δS36 (loop D), γW55/δW57 (loop E), γY111/δR113 (loop F), and γD174/δD180 (loop G) (*3*). Differences in the homologous non-α-subunit loops give the αγ and αδ sites different affinities for various agonists and competitive antagonists.

The α-conotoxins are short peptides found in cone snail venoms, which act as competitive antagonists of either muscle- or neuronal-type ACHRs (*4*). The primary structures of the three muscle-type ACHR-specific α-conotoxins used in this study are shown below

MI G−R−C−C−H−P−A−C-G−K−N−Y−S−C

GI E−C−C−N−P−A−C-G−R−H−Y−S−C

SI I−C−C−N−P−A−C-G−P−K−Y−S−C

These α-conotoxins all have two disulfide cross links, between the first and third cysteines and between the second and fourth cysteines, and amidated C terminals. Their published three-dimensional structures reveal that all three peptides have very similar backbone structures, despite the presence of proline at position 9 in SI, and fold into concave triangles or tripods with the three vertexes formed by the N-terminal/C-terminal junction, the proline at position 6 or 5 and the K10, R9, or P9 residue (*5*−*7*).

α-Conotoxins MI and GI display higher affinity for the αγ site on detergent-solubilized *Torpedo* ACHR than for the αδ site, while α-conotoxin SI is nonselective toward the two *Torpedo* sites (*8*, *9*). The molecular basis for this *Torpedo* selectivity is still uncertain. The midchain cationic residue on GI, R at position 9, was largely responsible for the αγ selectivity seen with GI (*10*, *11*). It was suggested but never confirmed that the homologous midchain cationic residue on MI, K at position 10, might also be the main determinant

† This work was supported by Grants NIH-MBRS-SO6-GM50695 and NIH-NCRR/SNRP-U54-NS39408.

* To whom correspondence should be addressed: Department of Biochemistry, Universidad Central del Caribe, Box 60-327, Bayamón, PR 00960. Fax 787-786-6285. E-mail: hannbio@coqui.net.

[1] Abbreviations: ACHR, nicotinic acetylcholine receptor; Bgt, α-bungarotoxin; I−Bgt, ^{125}I(Tyr 54)−α-bungarotoxin; TC, tubocurarine-*d*.

10.1021/bi030248b CCC: $27.50
Published on Web 09/08/2004

of the αγ selectivity of MI toward the *Torpedo* ACHR (*11*). On the receptor side, the Y at position 111 on loop F of the *Torpedo* γ subunit, as opposed to an R at the homologous position 113 on the δ subunit, was shown to be the main receptor determinant of the selective affinity of MI toward the αγ site on *Xenopus* oocyte-expressed *Torpedo* ACHR (*12*). It was hypothesized that the midchain cationic residues on GI and MI interact at close range with *Torpedo* γY111 to produce the high-affinity αγ binding (*11, 12*). The main purpose of this study was to address that hypothesis.

In this study, apparent affinity constants (IC_{50}s) of MI, GI, and SI and of their analogues, MIK10A, GIR9A, SIP9A, and SIP9R, for the two agonist sites on cell-expressed wild-type and γY111R, γY111A, and δR113Y mutant *Torpedo* ACHRs were determined. Thermodynamic double-mutant-cycle analysis was employed to see if pairs of the major selectivity-determinant residues interact. This is the first report to characterize α-conotoxin binding to wild-type and mutant *Torpedo californica* electrocyte ACHR transiently expressed on the cell surface of a human cell line. Such studies will help to clarify the molecular structure of the *Torpedo* ACHR, which has historically been a valuable model for understanding all other ligand-gated ion channels.

EXPERIMENTAL PROCEDURES

Materials. Plasmids containing individual wild-type *Torpedo californica* ACHR subunit cDNAs and an ampicillin-resistance gene in the pRBG4 expression vector were kindly provided by Dr. William Green, University of Chicago. Bacterial and cell culture media materials, antibiotics, tubocurarine-*d* (TC), and unlabeled α-bungarotoxin (Bgt) were from Sigma (St. Louis, MO). Other reagents were from Fisher (Cayey, PR). Synthetic α-conotoxins MI, GI, and SI were purchased from either Sigma or Bachem (King of Prussia, PA). α-Conotoxin analogues were synthesized at the Tufts University Core Facility (Boston, MA) using standard peptide synthesis methods. Peptides were allowed to air oxidize by stirring in phosphate-buffered saline containing 0.5 mM ethylenediaminetetraacetic acid (PBS-EDTA) buffer at pH 8.5 for 8 h, and then the buffer pH was readjusted to 7.5. All peptides were purified to >95% purity on HPLC. ^{125}I(Tyr 54)-α-bungarotoxin (I−Bgt) was purchased from Perkin−Elmer/New England Nuclear (Boston, MA).

Torpedo ACHR Subunit cDNA Plasmid Preparation. Plasmids were purified from transformed bacteria using a column method from QIAGEN (Valencia, CA), and the purity was confirmed by agarose gel electrophoresis. DH5α *E. coli* (Invitrogen, Carlsbad, CA) were transformed with individual wild-type *Torpedo* ACHR subunit plasmids. XL-1 Blue *E. coli* (Stratagene, La Jolla, CA) were transformed with individual mutant *Torpedo* ACHR subunit plasmids. Site-directed mutagenesis of wild-type *Torpedo* subunit cDNA was carried out using the appropriate mutagenic oligonucleotide primers and the Quik-Change Kit from Stratagene, and individual colonies selected for ampicillin resistance were grown up. Purified wild-type and mutant plasmids were sequenced at the Tufts University Core Facility to confirm each mutation.

Cell Transfection and Expression. Transfection of tsA201 cells (a human cell line kindly provided by Dr. William Green, University of Chicago) was carried out by modifying a previously published procedure (*13*). Cells were maintained in Dulbecco's modified Eagle medium containing 10% calf serum, 200 units/mL penicillin, and 200 μg/mL streptomycin. Within 20−24 h after a 1:5 trypsin split, cells were transfected with *Torpedo* ACHR subunit cDNAs in a ratio of 2:1:2.5:7.5 (α/β/γ/δ), using calcium phosphate precipitation. This same ratio was used for both wild-type and mutant subunits. Transfected cells were maintained for 4 h at 37 °C and 5% CO_2 and then washed twice with sterile 10 mM sodium phosphate buffer containing 137 mM NaCl and 3 mM KCl (CPBS) at pH 7.4 before adding fresh medium. Cells were incubated overnight at 37 °C and 5% CO_2 followed by incubation at 20 °C and 5% CO_2 for 4−6 days. Cells were returned to 37 °C and 5% CO_2 for 3 h immediately before harvesting. The transient expression of *Torpedo* ACHR on tsA201 cells was low-temperature-dependent as previously described with these cells (*13*) and with *Torpedo* ACHR stably expressed in mouse fibroblasts (*14*). Maximum expression was seen following 4−6 days at 20 °C, while no detectable expression was seen on cells maintained at 37 °C. Returning cells to 37 °C/5% CO_2 for 3 h prior to harvest increased expression by about 30%.

Cell-Surface-Binding Experiments. An I−Bgt equilibrium binding assay was used to determine maximum cell-surface expression of ACHR and to measure ACHR saturation. Briefly, cells were aspirated from plates following addition of CPBS containing 0.5 mM EDTA at pH 7.4 (CPBS-EDTA), and a cell suspension was prepared by pelleting and resuspending cells 3 times in the same buffer. After preincubation for 1 h, cells in CPBS-EDTA were incubated for 120 min in the presence of 5 nM I−Bgt. Kinetics studies (not shown) estimated that, in the absence of inhibitors, the time to 97% equilibrium in this system was approximately 90 min, so that the system is at equilibrium following this time period of incubation. Cells were then pelleted by centrifugation and washed twice with CPBS-EDTA. Specific I−Bgt binding was calculated by subtracting, from total binding, the nonspecific binding measured under the same conditions but in the presence of 500 nM unlabeled Bgt. In saturation-curve experiments, the total I−Bgt concentration was varied and unbound I−Bgt concentration was measured directly in the supernatant from the first centrifugation. Total protein in the cell suspensions was determined using the Bradford method (*15*), with bovine serum albumin as the standard, and ranged from 4 to 10 mg/mL. Competitive inhibitor concentration curves were constructed by measuring specific binding of I−Bgt with this same assay under near equilibrium conditions in the absence or presence of varying concentrations of inhibitor. It was estimated that, in the presence of inhibitors, the half-time to equilibrium in this system was 58 min, so that following 120 min of incubation the system is at about 76% of equilibrium.

Data Analysis. I−Bgt saturation binding data were fit to the following equation for binding of a radioligand to two equimolar, independent sites with apparent dissociation constants of K_1' and K_2':

$$B/B_t = 1/(1 + [(K_1'/L)/(1 + K_1'/K_2' + L/K_2')]) \quad (1)$$

where B is the concentration of specifically bound I−Bgt at unbound I−Bgt concentration L and B_t is the total concentration of available sites. Competition binding data with a single

inhibitor were fit to the following equation for mutually exclusive displacement from two independent sites:

$$y = [F/(1 + I/K_1)] + [(1 - F)/(1 + I/K_2)] \quad (2A)$$

where y is specifically bound I−Bgt at inhibitor concentration I normalized to the control (no inhibitor or very low inhibitor), F and $1 - F$ are the fractional amounts of each site present, and K_1 and K_2 are the apparent affinity constants (IC_{50}s) for the inhibitor at each site under the given experimental conditions.

Competition binding data with TC in the presence of a second inhibitor were fit to the following equation for mutually exclusive displacement from two equimolar independent sites by two competitive inhibitors I and J (*11*):

$$y = [0.5/(1 + \mathrm{I}/K_{1\mathrm{I}} + \mathrm{J}/K_{1\mathrm{J}})] + [0.5/(1 + \mathrm{I}/K_{2\mathrm{I}} + \mathrm{J}/K_{2\mathrm{J}})] \quad (2B)$$

This equation was used to identify peptide site selectivity when observed. Inhibition of specific I−Bgt binding by TC in the absence or presence of peptide at its IC_{50} concentration was normalized to the binding in the absence of TC or other inhibitors. Control data were fit to eq 2A, and the parameters, along with peptide parameters determined in separate experiments, were used to fit the binding data in the presence of peptide to eq 2B. The TC high-affinity ($\alpha\gamma$) site was made to coincide either with the peptide high-affinity site or with the peptide low-affinity site, and the best fit was identified.

The free energy change of binding (ΔG) was calculated from the apparent affinity constant (K)

$$\Delta G = +1.36 \log K \quad (3)$$

All curve fitting was performed using PSI−Plot version 6.51 software (Poly Software Int., Pearl River, NY) employing the Marquardt−Levenburg method. Each inhibitor curve involving a receptor mutation gave two affinity constants: one for the mutated site and one for the unmutated site. From the experimentally determined ΔG, the average $\Delta\Delta G$ at the unmutated sites was calculated to be $+0.11 \pm 0.36$ kcal/mol [mean ± standard deviation (SD)]. This corresponds to a maximum 95% confidence limit of about 0.83 kcal/mol or an affinity constant ratio of approximately 4. Therefore, only affinity constant changes larger than 4-fold were regarded as significant. This criterion was confirmed by statistical analysis of log-transformed data using a regular ANOVA method. Groups were compared using the nonparametric ANOVA Kruskal−Wallis test statistic. If significant differences ($p < 0.05$) were found, the Dunn's post-test was used to identify individual group differences. Statistical analyses were performed with GraphPad Prism version 3.0 (GraphPad Software Inc., San Diego, CA).

Thermodynamic double-mutant-cycle analysis was used to identify pairwise interactions between conotoxin peptide residues and ACHR subunit residues. To generate a double-mutant cycle for each pair of residues, the affinity constants and ΔG values for the four possible combinations of wild-type (W) and mutant (M) receptor and peptide (ΔG_{WW}, ΔG_{MW}, ΔG_{WM}, and ΔG_{MM}), where the first subscript letter indicates the receptor and the second subscript letter indicates the peptide, were determined under the same experimental conditions. These parameters were used to calculate the difference in free energy of binding for the two single mutants and the double mutant as

$$\Delta\Delta G_{\mathrm{MW}} = \Delta G_{\mathrm{MW}} - \Delta G_{\mathrm{WW}},$$
$$\Delta\Delta G_{\mathrm{WM}} = \Delta G_{\mathrm{WM}} - \Delta G_{\mathrm{WW}}, \quad \text{and}$$
$$\Delta\Delta G_{\mathrm{MM}} = \Delta G_{\mathrm{MM}} - \Delta G_{\mathrm{WW}}$$

and the interaction or "coupling" free energy $\Delta\Delta G_{\mathrm{INT}}$ (*16*) as

$$\Delta\Delta G_{\mathrm{INT}} = \Delta\Delta G_{\mathrm{MM}} - (\Delta\Delta G_{\mathrm{MW}} + \Delta\Delta G_{\mathrm{WM}}) \quad (5)$$

If the given pair of residues does not interact, $\Delta\Delta G_{\mathrm{INT}} = 0$; the individual mutant effects on the free energy of binding display additivity because their sum is equal to the effect of the double mutant ($\Delta\Delta G_{\mathrm{MM}} = \Delta\Delta G_{\mathrm{MW}} + \Delta\Delta G_{\mathrm{WM}}$). If the pair of residues interact, the sum of the individual mutant effects on the free energy of binding exceeds the effect of the double mutant and $\Delta\Delta G_{\mathrm{INT}}$ deviates from 0. The interaction may be either direct, through close contact, or indirect, through a structural perturbation or bridging through an intervening residue (*16*, *17*). In a protein−protein binding system, which does not include a functional measurement, such as that studied here, larger coupling energies (i.e., >1.0−1.5 kcal/mol) are generally due to direct contact (*16*, *18*). For this study, a $\Delta\Delta G_{\mathrm{INT}}$ deviation from 0 to at least ± 1.36 kcal/mol was established as evidence of interaction based on error analysis of the determination of this parameter as well as on the experience of others (*18*). This criterion was verified by calculating the average $\Delta\Delta G_{\mathrm{INT}}$ corresponding to the unmutated site for all 18 mutant cycles in this study, which should theoretically equal 0. This gave a value of -0.22 ± 0.45 kcal/mol (mean ± SD), which represents a 95% confidence limit of approximately 1.1 kcal/mol. Therefore, a minimal $|\Delta\Delta G_{\mathrm{INT}}|$ of 1.36 kcal/mol is a reasonably conservative criterion for close interaction. Atomic distances in the snail acetylcholine-binding protein (*19*) and in α-conotoxin MI (*5*) were determined from original structures deposited in the Protein Data Bank using the BioMedCache 6.0 program (Fujitsu, Beaverton, OR).

RESULTS

Characterization of tsA201 Cell-Expressed Wild-Type and Mutant Torpedo ACHRs. The radioligand, I−Bgt, binds with equal affinities at the two agonist sites located at the $\alpha\gamma$ and $\alpha\delta$ subunit interfaces on native *Torpedo californica* ACHR (*1*, *3*). Because this is the first report of site-specific inhibitor studies on tsA201 cell-surface-expressed *Torpedo* ACHR using competition with I−Bgt, it was necessary to confirm that the stoichiometry and the site nonselectivity of I−Bgt binding to cell-expressed wild-type and mutant ACHR are the same as with the native receptor. Specific binding of I−Bgt to wild-type ACHR was saturable above 10 nM (data not shown). Fitting the saturation data to eq 1 gave a single apparent dissociation constant of 1.2 ± 0.1 nM (mean ± SD, $n = 3$), which is consistent with either a single binding site or two or more sites having similar affinities. In contrast to Bgt, TC binds with stronger affinity to the *Torpedo* $\alpha\gamma$ site than to the $\alpha\delta$ site (*2*). Here, TC completely displaced I−Bgt from cell-expressed wild-type ACHR (see Figures 1C and 2C(i), control curve data). Fitting the TC data to eq 2A gave two distinct affinity constants, which were present in

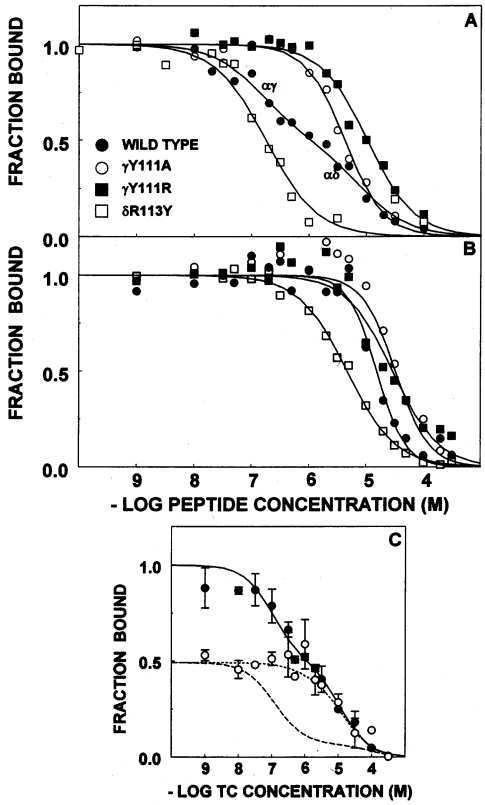

FIGURE 1: Inhibition of I−Bgt binding to tsA201 cell-expressed wild-type and mutant *Torpedo californica* ACHR by α-conotoxin MI (A) and its analogue, MIK10A (B). Cell suspensions were preincubated for 1 h in the absence or presence of peptide, then incubated for 2 h in the presence of 5 nM I−Bgt, and finally washed three times by centrifugation. Specific binding was calculated by subtracting the nonspecific binding, measured in the presence of 500 nM unlabeled Bgt and no other inhibitors, from the total binding and then normalized to specific binding measured in the absence of inhibitors ("fraction bound"). Each point represents the mean from 3 to 6 determinations. The legend in A identifies which receptor was expressed and is the same for B. Data were fit to eq 2A to generate the parameters in Table 1, which were used to produce the curves shown. Where site selectivity was observed, the upper (high-affinity) and lower (low-affinity) regions of the curve are labeled with the site that is the major determinant of the affinity. (C) Confirmation of α-conotoxin MI site selectivity on wild-type ACHR. Inhibition of specific I−Bgt binding, determined as described above, by TC at the indicated concentrations in the absence (●) or presence (○) of MI at 2 μM concentration was normalized to specific binding in the absence of TC or other inhibitors. Each point represents the mean ± standard error of the mean from 2 or 3 determinations. Control data were fit to eq 2A, and the parameters were used to generate the control curve (—). Data in the presence of peptide were fit to eq 2B using TC parameters from the control curve and peptide parameters determined in separate experiments (Table 1) with the TC high-affinity ($\alpha\gamma$) site made to coincide either with the peptide high-affinity site (···) or with the peptide low-affinity site (- - -).

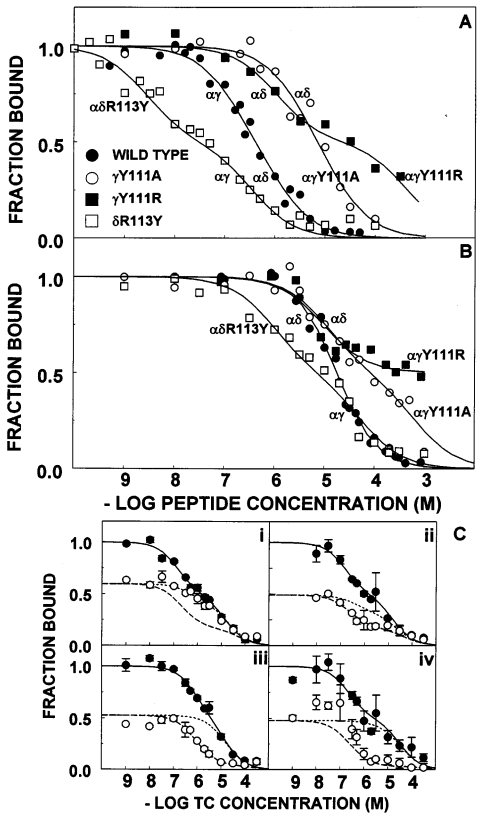

FIGURE 2: Inhibition of I−Bgt binding to tsA201 cell-expressed wild-type and mutant *Torpedo californica* ACHR by α-conotoxin GI (A) and its analogue, GIR9A (B). Specific binding of I−Bgt to cell-surface-expressed ACHR was measured as described in Figure 1 at the indicated peptide concentrations and normalized to binding measured in the absence of inhibitors. Each point represents the mean from 2 to 6 determinations. The legend in A identifies which receptor was expressed and is the same for B. Binding data were fit to eq 2A to generate the parameters in Table 1, which were used to produce the curves shown. Where site selectivity was observed, the upper (high-affinity) and lower (low-affinity) regions of the curve are labeled with the site that is the major determinant of the affinity. (C) Confirmation of GI site selectivity. Inhibition of specific I−Bgt binding by TC at the indicated concentrations was determined as described in the caption of Figure 1, except that I−Bgt binding to the (i) wild-type, (ii) γY111A mutant, (iii) γY111R mutant, or (iv) δR113Y mutant ACHR was measured in either the absence (●) or presence (○) of GI at (i) 300 nM, (ii) 3 μM, (iii) 12 μM, or (iv) 40 nM. Data in the presence of peptide were fit to eq 2B using TC parameters from the control curves and peptide parameters determined in separate experiments (Table 1) with the TC high-affinity ($\alpha\gamma$) site made to coincide either with the peptide high-affinity site (···) or with the peptide low-affinity site (- - -).

equimolar amounts ($F = 0.50 \pm 0.01$; five experiments). This is consistent with two I−Bgt-binding sites present in a 1:1 ratio. Two equimolar sites were also observed with TC competition curves on all three mutant ACHRs studied (parts ii, iii, and iv of Figure 2C). Therefore, the wild-type and mutant *Torpedo* ACHR molecules expressed on tsA201 cells retain the I−Bgt binding stoichiometry of two high-affinity sites per receptor molecule observed with the native receptor.

As mentioned above, the I−Bgt saturation studies indicated that the binding sites on wild-type ACHR have similar affinities. Data from homologous displacement experiments with wild-type ACHR were fit to eq 2A and also gave a single apparent affinity constant (24.5 ± 19.7 nM, $n = 3$). Together these results show that I−Bgt has the same affinity for the two sites on the cell-expressed wild-type *Torpedo* ACHR, at least within the sensitivity of this assay. Homologous displacement curves with mutant ACHRs did not differ from those with wild-type ACHR, giving single affinity constants in all three cases (γY111A = 31.9 ± 3.1 nM, WT = 32.9 ± 3.6 nM, $n = 2$; γY111R = 2.2 ± 0.2 nM, WT = 1.9 ± 0.1 nM, $n = 2$; and δR113Y = 39.7 ± 1.7 nM, WT = 38.6 ± 3.9 nM, $n = 2$). Therefore, these mutations do not measurably affect I−Bgt affinity for either the $\alpha\gamma$ or the $\alpha\delta$ site. This is the expected result, because the I−Bgt binding domains are located principally on the α subunits

Table 1: Binding Parameters of α-Conotoxins and Conotoxin Analogues for tsA201 Cell-Expressed *Torpedo californica* Wild-Type (WT) and Mutant ACHR Containing One Subunit with the Indicated Amino Acid Substitution[a]

		αγ site			αδ site			
toxin	ACHR	K (nM)	K/K_0	$-\Delta G$ (kcal/mol)	K (nM)	K/K_0	$-\Delta G$ (kcal/mol)	$K_{\alpha\delta}/K_{\alpha\gamma}$
MI	WT	147 ± 25	1	9.29	7956 ± 1389	1	6.94	54
	γY111A	4217 ± 268	29	7.31	4217 ± 268	0.53	7.31	1
	γY111R	10443 ± 790	71	6.77	10443 ± 790	1.3	6.77	1
	δR113Y	178 ± 31	1.2	9.18	178 ± 31	0.022	9.18	1
MIK10A	WT	15356 ± 1780	104	6.55	15356 ± 1780	1.9	6.55	1
	γY111A	32542 ± 2160	221	6.10	32542 ± 2160	4.1	6.10	1
	γY111R	28975 ± 5107	197	6.17	28975 ± 5107	3.6	6.77	1
	δR113Y	4698 ± 300	32	7.25	4698 ± 300	0.59	7.25	1
GI	WT	156 ± 27	1	9.26	1064 ± 182	1	8.12	7
	γY111A	15361 ± 5310	98	6.55	3253 ± 987	3.1	7.46	1/5
	γY111R	433732 ± 188678	2780	4.57	1076 ± 321	1.0	8.12	1/402
	δR113Y	345 ± 52	2.2	8.79	2.7 ± 0.5	0.0025	11.65	1/128
GIR9A	WT	17781 ± 934	114	6.46	17781 ± 934	17	6.46	1
	γY111A	619286 ± 153464	3970	4.36	11176 ± 2238	11	6.73	1/55
	γY111R	>850 000	>5449	<4.2	9449 ± 1749	8.9	6.83	<1/90
	δR113Y	52814 ± 9871	338	5.82	948 ± 203	0.89	8.19	1/56
SI	WT	3282 ± 351	1	7.46	3282 ± 351	1	7.46	1
	γY111A	6103 ± 509	1.8	7.09	6103 ± 509	1.8	7.09	1
	γY111R	11319 ± 752	3.4	6.73	11319 ± 752	3.4	6.73	1
	δR113Y	3453 ± 1991	1.1	7.43	10748 ± 6646	3.3	6.76	3
SIP9A	WT	9906 ± 490	3.0	6.80	9906 ± 490	3.0	6.80	1
	γY111A	7411 ± 397	2.2	6.98	7411 ± 397	2.2	6.98	1
	γY111R	158354 ± 22303	48	5.17	6817 ± 901	2.1	7.03	1/23
	δR113Y	19406 ± 7813	5.9	6.41	2721 ± 1089	0.83	7.57	1/7
SIP9R	WT	448 ± 130	0.14	8.63	5457 ± 1542	1.7	7.16	12
	γY111A	10676 ± 596	3.2	6.76	10676 ± 596	3.2	6.76	1
	γY111R	20710 ± 1761	6.3	6.36	20710 ± 1761	6.3	6.36	1
	δR113Y	995 ± 227	0.30	8.16	41.6 ± 10.7	0.013	10.04	1/24

[a] Apparent dissociation constant values (K) are IC_{50} values obtained by fitting experimental data to eq 2A. Shown are the mean ± SD from 3 to 9 measurements. When site selectivity was observed (unequal K values), the identity of the sites was determined with TC inhibition curves as described in the Experimental Procedures. K/K_0 is the ratio of the indicated K to that of the corresponding wild-type pair at the same site (K_0). Free energy of binding (ΔG) was calculated from eq 3. Only affinity constant changes larger than 4-fold ($\Delta\Delta G > 0.83$) are regarded as significant.

(*1*). This allows the use of I−Bgt to measure the affinity of other competitive inhibitors.

Also, the TC affinity constants for the mutated αγ or αδ sites did not differ significantly from those for the corresponding unmutated sites (αγ: WT = 169 ± 85 nM, γY111A = 277 ± 173 nM, γY111R = 594 ± 375 nM, δR113Y = 204 ± 29 nM, $p > 0.1$. αδ: WT = 20.6 ± 12.4 μM, γY111A = 20.7 ± 7.7 μM, γY111R = 12.7 ± 4.4 μM, δR113Y = 30.1 ± 2.4 μM, $p > 0.3$). This allows the use of TC to determine the site selectivity of other competitive inhibitors on the mutant receptors.

Cell-surface expression of wild-type *Torpedo* ACHR by tsA201 cells averaged 41.0 ± 21.5 fmol of receptor/mg of protein (mean ± SD of 21 transfections). This represents approximately 18 000 receptor molecules per cell. This expression level is similar to that previously reported for *Torpedo* ACHR transiently expressed in this same cell line (*13*). Average cell-surface expression of the γY111R mutant ACHR (27.8 ± 16.2 fmol of receptor/mg of protein; $n = 16$) was not significantly different from that of the wild type ($p > 0.05$). Expression of γY111A mutant ACHR (13.3 ± 2.4 fmol of receptor/mg of protein; $n = 6$) and of δR113Y mutant ACHR (11.4 ± 5.8 fmol of receptor/mg of protein; $n = 14$) were both significantly lower than that of wild-type ACHR ($p < 0.01$ and $p < 0.001$, respectively). Transfection with only α, β, and γ wild-type subunit cDNAs (2:1:5) or with only α, β, and δ wild-type subunit cDNAs (2:1:15) gave barely detectable surface expression (1−2 fmol of receptor/mg of protein). Mock transfection (no subunit cDNAs present) or transfection with only the α subunit cDNA produced no detectable specific I−Bgt binding.

α-*Conotoxin Binding to Cell-Expressed Torpedo ACHR.* α-Conotoxin MI completely displaced I−Bgt from both sites on the wild-type ACHR and showed over 50-fold stronger affinity for the αγ site than for the αδ site (Figure 1A and Table 1). This αγ site selectivity was confirmed with TC inhibition curves (Figure 1C). It should be noted that all of the apparent affinity constants (K values), which are listed in Table 1, are underestimates of the true affinity constants. This is because prolonged incubation was used in the peptide competition experiments rather than initial I−Bgt binding rate measurements. MI displayed weaker affinity for the mutant αγY111A and αγY111R sites than for the wild-type αγ site and stronger affinity for the mutant αδR113Y site than for the wild-type αδ site (Figure 1A). The γY111A, γY111R, and δR113Y substitutions eliminated the αγ site selectivity of MI, which was seen with the wild-type receptor. The analogue MIK10A also completely blocked I−Bgt binding to the wild-type receptor but showed the same, relatively weak, affinity for the αγ and αδ sites, which was similar to that of MI for the wild-type αδ site (Figure 1B and Table 1). The αγY111A, αγY111R, and αδR113Y substitutions had no significant effect on the affinity of MIK10A.

α-Conotoxin GI completely displaced I−Bgt from wild-type ACHR but showed only a 7-fold stronger affinity for the αγ site than for the αδ site (Figure 2A and Table 1). The affinities of GI and MI for the wild-type αγ site were

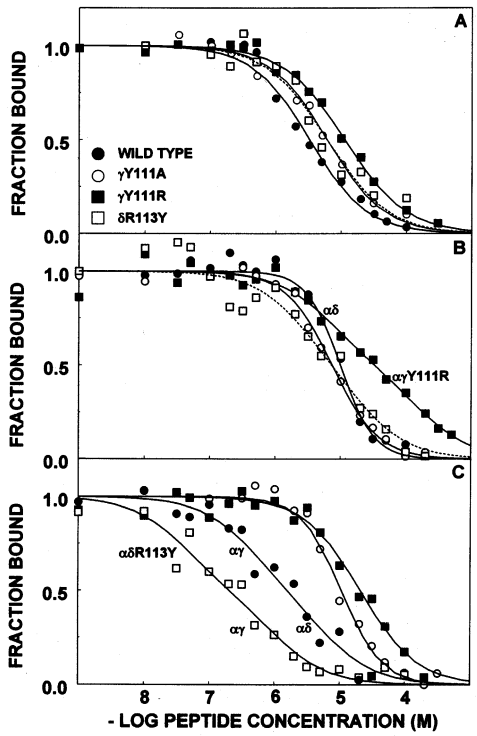

FIGURE 3: Inhibition of I−Bgt binding to tsA201 cell-expressed wild-type and mutant *Torpedo californica* ACHR by α-conotoxin SI (A) and its analogues, SIP9A (B) and SIP9R (C). Specific binding of I−Bgt to cell-surface-expressed ACHR at the indicated peptide concentrations was measured and normalized as described in Figure 1. Each point represents the mean from 2 or 3 determinations. The legend in A identifies which receptor was expressed and is the same for B and C. Data were fit to eq 2A to generate the parameters in Table 1, which were used to produce the curves shown. The curves corresponding to the δR113Y mutant in A and B are shown as dotted lines. Where site selectivity was observed, the upper (high-affinity) and lower (low-affinity) regions of the curve are labeled with the site that is the major determinant of the affinity.

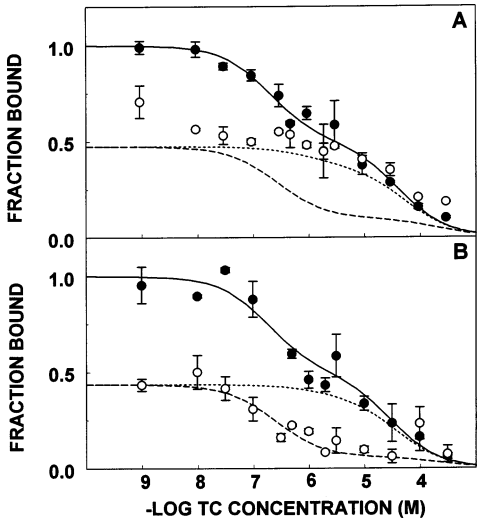

FIGURE 4: Confirmation of SIP9R site selectivity. Inhibition of specific I−Bgt binding by TC at the indicated concentrations was determined as described in the caption of Figure 1, except that specific I−Bgt binding to the (A) wild-type or (B) δR113Y mutant ACHR was measured in either the absence (●) or presence (○) of SIP9R at (A) 2 μM or (B) 322 nM concentration. Data in the presence of peptide were fit to eq 2B using TC parameters from the control curves and peptide parameters determined in separate experiments (Table 1) with the TC high-affinity (αγ) site made to coincide either with the peptide high-affinity site (···) or with the peptide low-affinity site (- - -).

similar, but GI displayed relatively stronger affinity than MI for the αδ site. GI showed weaker affinity for the αγY111A site than for the wild-type αγ site but displayed much weaker affinity for the αγY111R site than for the wild-type αγ site. The affinities of GI for both of these mutant sites were weaker than its affinity for the unmutated αδ site, resulting in GI having αδ site selectivity on these two mutant receptors. GI displayed much stronger affinity for the αδR113Y site than for the wild-type αδ site. The affinity of GI for the αδR113Y site was even stronger than that for the unmutated αγ site, giving GI a 100-fold αδ site selectivity with this amino acid substitution present. The site selectivities of GI were all confirmed with TC inhibition curves (Figure 2C). The GI analogue, GIR9A, also completely blocked I−Bgt binding to wild-type ACHR but showed the same affinities toward the αγ and αδ sites, which were weaker than the affinity of GI for the wild-type αδ site (Figure 2B and Table 1). GIR9A also showed weaker affinity for the αγY111A than for the wild-type αγ site, much weaker affinity for the αγY111R site than for the wild-type αγ site, and stronger affinity for the αδR113Y site than for the wild-type αδ site.

α-Conotoxin SI was nonselective toward the wild-type αγ and αδ sites, showing the same relatively weak affinity for both (Figure 3A and Table 1). The affinity of SI for each site was not affected appreciably by any of the three mutations studied. Analogue SIP9A resembled SI in being nonselective toward the wild-type αγ and αδ sites, with an affinity similar to that of SI (Figure 3B and Table 1). Also, SIP9A was unaffected by the γY111A and δR113Y substitutions. SIP9A displayed weaker affinity for the mutant αγY111R site than for the wild-type αγ site. In contrast to SI and SIP9A, the analogue SIP9R more closely resembled MI or GI in displaying stronger affinity for the wild-type αγ site than for the wild-type αδ site (Figure 3C and Table 1). SIP9R also showed weaker affinity for the mutant αγY111A and αγY111R sites than for the wild-type αγ site and stronger affinity for the mutant αδR113Y site than for the wild-type αδ site. Like MI but unlike GI, SIP9R showed the same affinity for the αγY111A, αγY111R, and unmutated αδ sites. Like GI but unlike MI, SIP9R displayed selectively stronger affinity for the mutant αδR113Y site than for the unmutated αγ site. The site selectivities of SIP9R were confirmed with TC inhibition curves (Figure 4).

Table 2 summarizes the coupling energies determined for 18 double-mutant cycles. A strong pairwise interaction is seen between γY111 and K10 on MI (cycles 1 and 2), while the coupling energy for cycle 3 did not differ from the unmutated αδ site. This shows that K10 on MI interacts, probably at close range, with the aromatic ring of γY111 in the *Torpedo* αγ site to stabilize the high-affinity complex. Pairwise interaction between the mutant δR113Y and K10 on MI is also seen (cycle 4), indicating that K10 interacts with Y at position 113 on the δ subunit in the mutant *Torpedo* αδR113Y site to stabilize the high-affinity MI−δR113Y complex. In contrast, mutant-cycle analysis with GI and GIR9A using the γY111A mutant gave a coupling energy, which was similar to that for the unmutated αδ site (cycle 5), indicating that R9 on GI and γY111 do not interact to stabilize the GI−αγ complex. A possible interaction

Table 2: Coupling Free Energies from Double-Mutant-Cycle Analysis of α-Conotoxin Binding Data Presented in Table 1[a]

		αγ site	αδ site
	double-mutant cycle	$\Delta\Delta G_{INT}$ (kcal/mole)	$\Delta\Delta G_{INT}$ (kcal/mole)
1.	WT/γY111A/MI/MIK10A	−1.53**	+0.82
2.	WT/γY111R/MI/MIK10A	−2.14**	+0.21
3.	γY111A/γY111R/MI/MIK10A	−0.61**	−0.61
4.	WT/δR113Y/MI/MIK10A	−0.81	+1.54**
5.	WT/γY111A/GI/GIR9A	−0.61**	−0.93
6.	WT/δR113Y/GI/GIR9A	+0.17	+1.80**
7.	WT/γY111A/SI/SIP9R	+1.50**	+0.03
8.	WT/γY111R/SI/SIP9R	+1.54**	+0.07
9.	γY111A/γY111R/SI/SIP9R	+0.04**	+0.04
10.	WT/δR113Y/SI/SIP9R	+0.44	−3.58**
11.	WT/γY111A/SIP9R/SIP9A	−2.05**	−0.58
12.	WT/γY111R/SIP9R/SIP9A	−0.64**	−1.03
13.	γY111A/γY111R/SIP9R/SIP9A	+1.41**	−0.45
14.	WT/δR113Y/SIP9R/SIP9A	−0.08	+2.11**
15.	WT/γY111A/SI/SIP9A	−0.55**	−0.55
16.	WT/γY111R/SI/SIP9A	+0.90**	−0.96
17.	γY111A/γY111R/SI/SIP9A	+1.45**	−0.41
18.	WT/δR113Y/SI/SIP9A	+0.36	−1.47**

[a] Coupling free energy ($\Delta\Delta G_{INT}$) was calculated from eq 5 as defined in the Experimental Procedures using the parameters presented in Table 1. In each cycle, the mutated site is indicated by **. For this study, a $\Delta\Delta G_{INT}$ deviation from 0 to at least ±1.36 kcal/mol was established as evidence of interaction based on error analysis of the determination of this parameter as well as on the experiences of others (*18*).

between GIR9 and γY111 could not be analyzed with the γY111R/GIR9A mutant cycle because the affinity constant of GIR9A for the αγY111R site exceeded the solubility limit of the peptide. However, the large affinity constant suggests that the binding energy differences in this cycle are also additive and, therefore, that γY111 and GIR9 do not interact. In contrast to the αγ site, pairwise interaction between δR113Y and R9 on GI is observed (cycle 6). This indicates that R9 on GI interacts at close range with Y substituted at δ113 to account for the increased affinity of GI at the mutated αδR113Y site, resembling MI in this respect. Pairwise interaction between R9 on SIP9R and γY111 is seen in three of four cycles (cycles 7, 8, and 11). This together with the small coupling energy using SIP9R and SI with both γ111 mutants (cycle 9) indicates that the aromatic ring of γY111 interacts at close range with R9 on SIP9R to stabilize the αγ−SIP9R complex. A pairwise interaction is also seen between Y substituted at δ113 and R9 on SIP9R (cycles 10 and 14). Therefore, R9 on SIP9R, like R9 on GI and K10 on MI, interacts, probably at close range, with δR113Y to stabilize the complex in the αδR113Y site. A total of 6 of the 18 double-mutant pairs shown in Table 2 display coupling energies well below the threshold of ±1.36 kcal/mol, which supports the conclusion that the identified pairwise interactions are through direct contact and are not indirect interactions via a structural perturbation or an intervening residue.

DISCUSSION

α-Conotoxin-Binding Sites on the Cell-Expressed Torpedo ACHR. The substitution of A for K at position 10 of MI converted this peptide into a nonselective ligand with an affinity similar to the affinity of MI for the αδ site. This confirms an earlier prediction, which was based on studies with GI and SI position 9 analogues, that the homologous K10 would be a major determinant of the selective high affinity of MI for the αγ site on *Torpedo* ACHR (*11*). The findings with MI also support the conclusion made in the only other report describing MI inhibition of I−Bgt binding to cell-expressed wild-type and mutant *Torpedo* ACHRs that the residue difference at homologous positions γY111 and δR113 is the main receptor determinant of the selective high affinity of MI toward the *Torpedo* αγ site (*12*). The present study further shows that this residue difference is also a major determinant of the selective αγ high affinity of both GI and the SI analogue, SIP9R.

It was hypothesized that the midchain cationic residues on MI and GI interact directly with *Torpedo* γY111 to stabilize the high-affinity complexes of these two peptides at the wild-type αγ site (*11*, *12*). The mutant-cycle analyses in this study support this hypothesis only in the case of MI. The interaction between the aromatic ring of γY111 and MIK10 is entirely responsible for the higher affinity of MI at the αγ site and contributes approximately 2 kcal/mol to the Δ*G* of binding. This suggests that γY111 and MIK10 are less than 7 Å from each other (*18*). In the *Lymnea stagnalis* acetylcholine-binding protein subunit the C_α of the residue corresponding to *Torpedo* γY111 (V106) is within 20 Å of the C_α of residue W53, which is homologous to *Torpedo* γW55 and forms one wall of the agonist-binding cage (*19*). MI, which measures over 22 Å from the ϵ-amino nitrogen on K10 to the outer guanidinium nitrogens on R2 (*5*), probably binds in the αγ interface with residue K10 interacting directly with γY111 to block access of the agonist to its binding cage. Like MI, the SI analogue, SIP9R, also forms a high-affinity complex with the αγ site through a close interaction between its cationic midchain residue and the aromatic ring of γY111. This bond contributes about 1.8 kcal/mol toward stabilizing the αγ−SIP9R complex. Therefore, MI and SIP9R utilize a common anchor point in the αγ site.

Because γY111 interacts at close range with K10 on MI and with R9 on SIP9R, it is unexpected that it does not also interact with R9 on GI, in view of the similar three-dimensional structures of these three peptides (*5*−*7*). Because γY111 and R9 are both major determinants of the αγ high affinity of GI, it is likely that both residues are involved in stabilizing the GI−αγ high-affinity complex through separate interactions. This means that GI must bind in a different orientation than either MI or SIP9R in the *Torpedo* αγ site. The fact that equivalent parts of two very similar peptides (GI and SIP9R) contribute differently to binding at the same receptor site is not surprising because GI and SI (and probably also SIP9R) have "markedly different" surface charge distributions (*7*). It was recently reported that TC and metocurine, competitive antagonists with very similar structures, bind in different orientations at the acetylcholine-binding site of the human ACHR (*20*) and of the snail acetylcholine-binding protein (*21*). The present study confirms the observation in those papers that, although the structures of two ligands may appear very similar, it cannot be assumed that their interactions and orientations in a given binding domain will be the same.

The substitution of Y for R at position 113 on the *Torpedo* δ subunit converted the αδ site into a high-affinity site for MI, GI, and SIP9R. Mutant-cycle analyses showed that this involved pairwise interactions between the introduced Y

residue and K10 on MI and R9 on both GI and SIP9R. Therefore, all three peptides bind in the mutant αδR113Y site with their midchain cationic residues close to δY113 and probably block agonist access to its binding site in the αδ interface in a manner analogous to MI and SIP9R at the αγ site. In the case of MI, the putative K10−δY113 interaction contributes approximately 2 kcal/mol, which is similar to the contribution of the K−Y interaction at the αγ site. It was previously suggested that repulsive forces between the positive charges on K10 of MI and on δR113 might be responsible for the much weaker binding of MI in the *Torpedo* αδ site (*12*). The finding in this study that MI and MIK10A have similar affinities for the αδ site shows that the weaker affinity of MI in the αδ site is not due to electrostatic repulsion but instead is simply due to the absence of the K−Y bond, which exists only in the αγ site. The overall findings that the affinities of MI for the mutated sites equaled its affinities for the unmutated sites and that the affinities of MIK10A for the two sites were equal regardless of whether one of the sites was mutated demonstrate that the residues in the αγ and αδ sites with which MI interacts, other than at γ111/δ113, are either the same or similar enough to exert equivalent effects on MI in the two sites. This is only possible if MI binds to the *Torpedo* ACHR with the same orientation in the two sites.

SIP9R probably also binds with the same orientation in the αγ and αδ sites, because SIP9R anchors to the homologous γ111/δ113 residue in both the αγ and αδR113Y sites, its affinities for the αγY111A and αγY111R sites equaled its affinity for the unmutated αδ site, and the affinities of SI for the αγ and αδ sites were equal, regardless of whether one of the sites was mutated. However, unlike MI, the affinity of SIP9R for the αδR113Y site exceeded its affinity for the unmutated αγ site by nearly 2 kcal/mol. This suggests that substitution of Y for R at position δ113 allows at least one additional residue, present only on δ, to interact with SIP9R to increase its affinity. This putative additional interaction probably involves R9, because this same effect is not seen at the αδR113Y site with either SI or SIP9A.

The finding that R9 on GI interacts closely with δR113Y but not with γY111 means that GI must bind with different orientations in the two *Torpedo* sites. As with SIP9R, the affinity increase for GI between αδ and αδR113Y is also quite large ($\Delta\Delta G = 3.53$ kcal/mol) and is probably not entirely due to the R−Y interaction, because the GI analogue, GIR9A, also gained substantial affinity ($\Delta\Delta G = 1.73$ kcal/mol) between αδR113 and αδR113Y. This suggests that substituting Y for R at δ113 allows additional bonds to form between one or more GI residues (other than R9) and one or more residues in the αδR113Y site.

Difference between the α-Conotoxin MI High-Affinity Binding Sites on Torpedo and Embryonic Mouse Muscle ACHRs. This study shows how the molecular basis for the high affinity of MI on *Torpedo* ACHR is different from that on the embryonic mouse muscle ACHR. The ACHR from *Torpedo* electric organ is often referred to as a "muscle-type" ACHR because of its location in a peripheral, muscle-derived organ and its structural and functional similarities to vertebrate muscle ACHRs. However, the α-conotoxin-binding sites on the *Torpedo* ACHR and on the embryonic mouse muscle ACHR are different. In contrast to *Torpedo*, MI, GI, and even SI display selectively higher affinity for the αδ site on the mouse muscle ACHR (*9*). Hydrophobic interactions involving several residues, including δY113, the homologue of *Torpedo* γY111, stabilize the high-affinity MI−αδ complex (*22*). However, mouse δY113 does not interact with K10 on MI. In contrast, the present study shows that the cationic residue K10 binds directly with the aromatic ring of γY111 to produce the αγ high affinity of MI on *Torpedo* ACHR. While hydrophobic forces may be involved in stabilizing the *Torpedo* αγ−MI complex, they do not produce the selective high affinity observed. Therefore, not only are different subunit interfaces involved, but also the molecular interactions that occur within the interfaces are different. It is intriguing that the same property, high-affinity competitive antagonist inhibition at one of two available agonist sites on homologous proteins, is produced by two distinct molecular mechanisms. From a biological viewpoint, this may reflect separate evolutionary pressures on the cone snail: toward predation in the case of the muscle-derived electric organ receptor, which comes from a marine fish species more closely related to the natural prey of these fish-hunting molluscs, and as defense against predation in the case of the muscle receptor from a mammal, which is not related to a natural prey of the cone snails but is more closely related to predatory mollusc-hunting marine mammals.

ACKNOWLEDGMENT

The authors thank Dr. William Green, University of Chicago, for providing tsA201 cells and *Torpedo* ACHR subunit cDNAs and consulting on this project and Dr. Catharine Reinitz, University of Wisconsin, whose efforts helped establish the transfection methodologies in this lab. The authors also thank Migdalia Bonilla and Aimee Berolo for their excellent technical assistance.

REFERENCES

1. Karlin, A. (2002) Emerging structure of the nicotinic acetylcholine receptors, *Nat. Rev. 3*, 102−114.
2. Pedersen, S. E., and Cohen, J. B. (1990) d-Tubocurarine binding sites are located at α-γ and α-δ interfaces of the nicotinic acetylcholine receptor, *Proc. Natl. Acad. Sci. U.S.A. 87*, 2785−2789.
3. Sine, S. M. (2002) The nicotinic receptor ligand-binding domain, *J. Neurobiol. 53*, 431−446.
4. McIntosh, J. M., Santos, A. D., and Olivera, B. M. (1999) *Conus* peptides targeted to specific acetylcholine receptor subtypes, *Annu. Rev. Biochem. 68*, 59−88.
5. Gouda, H., Yamazaki, K., Hasegawa, J., Kobayashi, Y., Nishiuchi, Y., Sakakibara, S., and Hirano, S. (1997) Solution structure of α-conotoxin MI determined by ^{1}H NMR spectroscopy and molecular dynamics simulation, *Biochim. Biophys. Acta 1343*, 327−334.
6. Guddat, L. W., Martin, J. L., Shan, L., Edmundson, A. B., and Gray, W. R. (1996) Three-dimensional structure of the α-conotoxin GI at 1.2 Å resolution, *Biochemistry 35*, 11329−11335.
7. Benie, A. J., Whitford, D., Hargittai, B., Barany, G., and Janes, R. W. (2000) Structure solution of α-conotoxin SI, *FEBS Lett. 476*, 287−295.
8. Hann, R. M., Pagán, O. R., and Eterović, V. A. (1994) The α-conotoxins GI and MI distinguish between the nicotinic acetylcholine receptor agonist sites while SI does not, *Biochemistry 33*, 14058−14063.
9. Groebe, D. R., Dumm, J. M., Levitan, E. S., and Abramson, S. N. (1995) α-Conotoxins selectively inhibit one of the two acetylcholine binding sites of nicotinic receptors, *Mol. Pharmacol. 48*, 105−111.
10. Groebe, D. R., Gray, W. R., and Abramson, S. N. (1997) Determinants involved in the affinity of α-conotoxins GI and SI

for the muscle subtype of nicotinic acetylcholine receptors, *Biochemistry 36*, 6469−6474.
11. Hann, R. M., Pagán, O. R., Gregory, L. M., Jacome, T., and Eterović, V. A. (1997) The 9-arginine residue of α-conotoxin GI is responsible for its selective high affinity for the αγ agonist site on the electric organ acetylcholine receptor, *Biochemistry 36*, 9051−9056.
12. Chiara, D. C., Xie, Y., and Cohen, J. B. (1999) Structure of the agonist-binding sites of the *Torpedo* nicotinic acetylcholine receptor: Affinity labeling and mutational analyses identify γtyr111/δarg113 as antagonist affinity determinants, *Biochemistry 38*, 6689−6698.
13. Eertmoed, A. L., Vallejo, Y. F., and Green, W. N. (1998) Transient expression of heteromeric ion channels, *Methods Enzymol. 293*, 564−585.
14. Claudio, T., Green, W. N., Hartman, D. S., Hayden, D., Paulson, H. L., Sigworth, F. J., Sine, S. M., and Swedlund, A. (1987) Genetic reconstitution of functional acetylcholine receptor channels in mouse fibroblasts, *Science 238*, 1688−1694.
15. Bradford, M. M. (1976) A rapid and sensitive method for the quantitation of microgram quantities of protein utilizing the principle of protein-dye binding, *Anal. Biochem. 72*, 248−254.
16. Wells, J. A. (1990) Additivity of mutational effects in proteins, *Biochemistry 29*, 8509−8517.
17. Horovitz, A., and Fersht, A. R. (1990) Strategy for analyzing the cooperativity of intramolecular interactions in peptides and proteins, *J. Mol. Biol. 214*, 613−617.
18. Schreiber, G., and Fersht, A. R. (1995) Energetics of protein−protein interactions: Analysis of the barnase-barstar interface by single mutations and double-mutant cycles, *J. Mol. Biol. 248*, 478−486.
19. Brejc, K., van Dijk, W. J., Klaassen, R. V., Schuurmans, M., van der Oost, J., Smit, A. B., and Sixma, T. K. (2001) Crystal structure of an ACh-binding protein reveals the ligand-binding domain of nicotinic receptors, *Nature 411*, 269−276.
20. Wang, H.-L., Gao, F., Bren, N., and Sine, S. M. (2003) Curariform antagonists bind in different orientations to the nicotinic receptor ligand-binding domains, *J. Biol. Chem. 278*, 32284−32291.
21. Gao, F., Bren, N., Little, A., Wang, H.-L., Hansen, S. B., Talley, T. T., Taylor, P., and Sine, S. M. (2003) Curariform antagonists bind in different orientations to the acetylcholine-binding protein, *J. Biol. Chem. 278*, 23020−23026.
22. Bren, N., and Sine, S. M. (2000) Hydrophobic pairwise interactions stabilize α-conotoxin MI in the muscle nicotinic acetylcholine receptor binding site, *J. Biol. Chem. 275*, 12692−12700.

BI030248B